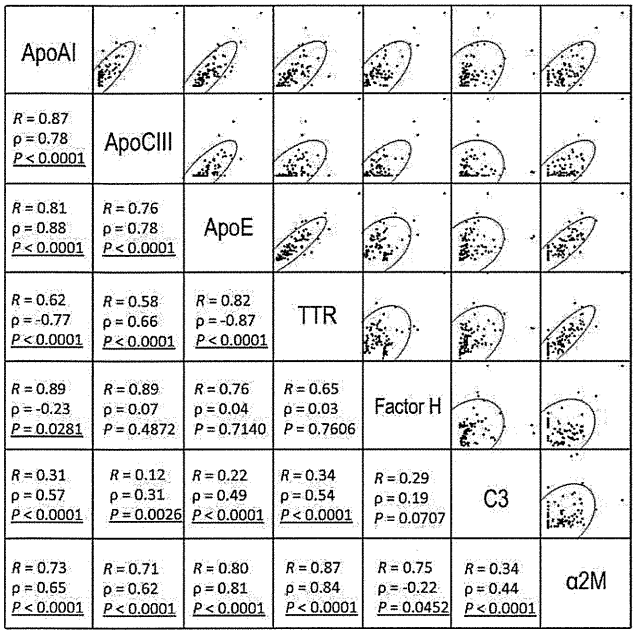

Figure 2. Multivariate correlations between the analyte concentrations. Scatterplot matrices are on the *right*, and statistical values appear on the *left*. Concentrations of Apo AI, ApoCIII, ApoE, TTR, complement component C3, and α2M were highly correlated with each other ($P < 0.0001$). The level of complement factor H was correlated only with the levels of Apo AI and α2M ($P < 0.05$).

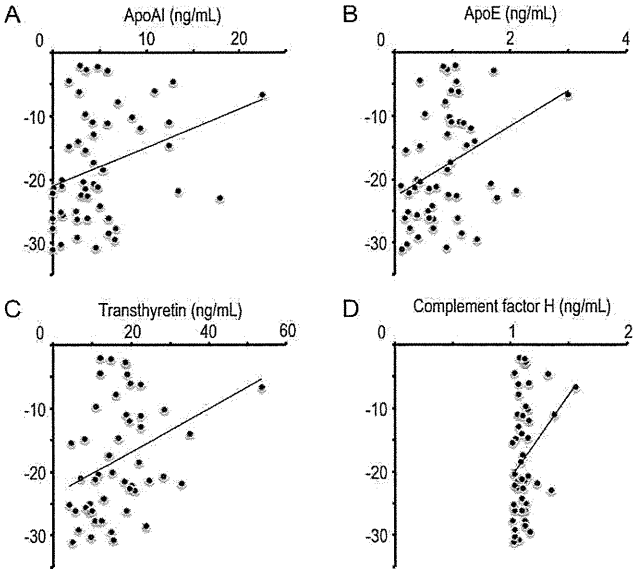

Figure 3. Correlations of the MD in Humphrey visual field analysis with aqueous Apo A1 (**A**), ApoE (**B**), TTR (**C**), and complement factor H (**D**). The *x*-axes represent the levels of analytes, and the *y*-axes represent the MD values (dB). *Scatterplots* show that the MD values correlated positively with the levels of Apo AI, ApoE, TTR, and complement factor H ($P = 0.0258$, 0.0117, 0.0081, and 0.0271, respectively), and their coefficients of correlation were 0.31, 0.35, 0.37, and 0.31, respectively.

revealed high correlations among levels of Apo AI, ApoCIII, ApoE, TTR, complement component C3, and α2M in these cases ($P < 0.0001$ in all combinations except for complement component C3-ApoCIII, $P = 0.0026$). The level of complement factor H, however, was weakly correlated only with levels of Apo AI and α2M ($P = 0.0281$ and 0.0452, respectively).

Relationships of IOP and Visual Field Severity to Levels of AD-Related Proteins in the Aqueous Humor of OAG Eyes

Additional analyses were performed to determine clinical characteristics that were associated with levels of AD-related proteins in the aqueous humor obtained from OAG patients. Statistical analysis revealed that age, preoperative IOP value, number of glaucoma eye drops, and duration of glaucoma therapy were not significantly correlated with the level of any protein measured (data not shown). The mean deviation (MD) value in the Humphrey visual field analysis correlated positively with levels of Apo AI, ApoE, TTR, and complement factor H ($P = 0.0258$, 0.0117, 0.0081, and 0.0271, respectively), although the correlations were not strong (coefficients of correlation were 0.31, 0.35, 0.37, and 0.31, respectively) (Fig. 3).

Discussion

The aqueous humor provides nutrients to avascular tissues, such as the lens, cornea, and trabecular meshwork, in the anterior ocular segment and, in humans, drains mainly through the conventional outflow pathway. The aqueous humor contains various biologically active factors, such as cytokines and growth factors, and some of these factors may be associated with the pathophysiology of glaucoma.[15–19] The multiplex bead immunoassay is a recently developed technique that is highly sensitive compared with the enzyme-linked immunosorbent assay,[20] and it allows simultaneous measurement of the levels of numerous cytokines and growth factors in a small aqueous humor sample.[21,22] Past studies, including ours, reported that the new technique can be a useful and reliable method for assessing biologically active factors in the aqueous humor samples.[2,23–25] Our present investigation revealed, via the multiplex bead immunoassay, detectable levels of AD-related biomarkers, Apo AI, ApoCIII, ApoE, TTR, complement factor H, complement component C3, and α2M, in human aqueous humor samples obtained from patients with cataract or OAG.

In the present study, human aqueous humor samples obtained from both ExG and POAG patients had elevated levels of Apo AI, ApoCIII, ApoE, TTR, and α2M. Elevated levels of these biomarkers cannot be explained simply by an impaired blood–aqueous barrier by following reasons. Firstly, there were no significant differences in any of the factors measured in the present study between POAG and ExG, though ExG eyes were thought to have more disrupted blood–aqueous barrier compared with POAG. Secondly, levels of complement factor H and complement component C3 were not elevated in OAG patients compared with the controls. Finally, the levels of α2-macroglobulin and complement factor H were negatively correlated with each other ($P = 0.0452$). Increased local production in the glaucomatous anterior ocular segment may be another explanation. Although the ciliary epithelium reportedly expressed some of the analytes,[26] their physiologic roles in the anterior ocular segment remain elusive.

Statistical analysis revealed that number of glaucoma eye drops and duration of glaucoma therapy were not significantly correlated with the level of any protein measured. However,

the effects of pre-operative glaucoma eye drops might be masked, because many of glaucoma patients had received full medication before surgery. For instance, 47 (90.0%), 48 (92.3%), and 46 (88.5%) of 52 glaucoma patients received eye drops of β-blockers, prostaglandin analogues, and carbonic anhydrase inhibitors at the time of surgery, respectively. Thus, we did not have enough sample number of glaucoma patients without eye drops, and therefore we cannot exclude the possibility that glaucoma eye drops affect the aqueous levels of AD-related biomarkers.

The present study is the first to provide evidence of the correlation between aqueous levels of AD-related biomarkers and the severity of visual field defects in OAG patients. The MD value correlated positively with the aqueous levels of Apo AI, ApoE, TTR, and complement factor H ($P = 0.0258$, 0.0117, 0.0081, and 0.0271, respectively). However, coefficients of correlation were relatively low (<0.4), and therefore additional studies with large sample sizes are needed to conclude that aqueous levels of those biomarkers truly reflect the severity of the visual field defect.

Apos make lipids water soluble by binding, thereby forming lipoproteins transporting lipids. Although the *APOE* genotype was reportedly related to AD-associated risk,[4] the level of ApoE was not elevated in the CSF.[27–29] In contrast, previous results about the association of the *APOE* genotype with OAG were controversial,[30,31] and in the present study and a past study, the aqueous humor of OAG eyes demonstrated an increased level of ApoE.[11] Other Apos were also found, by using proteomics techniques, to be related to AD.[32] One interesting result was that ApoE-containing lipoproteins had the potential to protect retinal ganglion cells against glutamate-induced apoptosis.[33] In that study, α2M, another AD-related biomarker whose level was increased in OAG eyes in our study here, interfered with the neuroprotective effects of ApoE-containing lipoproteins, because ApoE and α2M utilize a common receptor, the low density lipoprotein receptor-related protein 1. In addition, levels of α2M were high in both human POAG eyes and rat glaucoma model eyes,[14] and α2M had neurotoxic effects on retinal ganglion cells.[34,35] Although the exact pathophysiologic roles of ApoE and α2M in glaucomatous eyes have not been fully clarified, increased levels of ApoE and α2M in the aqueous humor of glaucomatous eyes suggest a link between these proteins and glaucoma pathophysiology.

TTR (which was previously called prealbumin) transports thyroxine and retinol and was reported to be a potential biomarker of AD, although past reports about AD-related changes in TTR in CSF have been controversial.[27,36] In the eye, TTR is expressed in the ciliary epithelium and RPE,[26,37,38] and eyes with POAG contain more TTR in the aqueous humor compared with cataractous eyes.[12,13] In the present study, the aqueous level of TTR increased not only in eyes with POAG, but also in eyes with ExG. In contrast, Bouhenni et al. reported that the level of TTR decreased in the aqueous humor of eyes with primary congenital glaucoma.[39] A well-known TTR-related disease is familial amyloid polyneuropathy,[40–42] and patients with this disease often develop secondary glaucoma.[43] Data therefore suggest that, although the role of aqueous TTR in glaucoma pathophysiology is unclear, TTR might be related to glaucomatous changes in the anterior chamber.

In conclusion, the findings of our study described here revealed that both ExG patients and POAG patients manifested elevated levels of biomarkers of AD, such as apolipoproteins, α2M, and TTR, in the aqueous humor. Levels of those analytes correlated with each other and may reflect the severity of glaucoma.

Acknowledgments

Supported by the Japan Society for the Promotion of Science KAKENHI Grant numbers 23390403, 23659814, 23791993, and 23791994.

Disclosure: **T. Inoue**, None; **T. Kawaji**, None; **H. Tanihara**, None

References

1. Quigley HA, Broman AT. The number of people with glaucoma worldwide in 2010 and 2020. *Br J Ophthalmol.* 2006;90:262–267.
2. Inoue T, Kawaji T, Inatani M, Kameda T, Yoshimura N, Tanihara H. Simultaneous increases in multiple proinflammatory cytokines in the aqueous humor of pseudophakic glaucomatous eyes. *J Cataract Refract Surg.* 2012;38:1389–1397.
3. Fagan AM, Perrin RJ. Upcoming candidate cerebrospinal fluid biomarkers of Alzheimer's disease. *Biomark Med.* 2012;6:455–476.
4. Kim J, Basak JM, Holtzman DM. The role of apolipoprotein E in Alzheimer's disease. *Neuron.* 2009;63:287–303.
5. Buxbaum JN, Ye Z, Reixach N, et al. TTR protects Alzheimer's mice from the behavioral and biochemical effects of Abeta toxicity. *Proc Natl Acad Sci U S A.* 2008;105:2681–2686.
6. Li X, Masliah E, Reixach N, Buxbaum JN. Neuronal production of TTR in human and murine Alzheimer's disease: is it protective? *J Neurosci.* 2011;31:12483–12490.
7. Bayer AU, Keller ON, Ferrari F, Maag KP. Association of glaucoma with neurodegenerative diseases with apoptotic cell death: Alzheimer's disease and Parkinson's disease. *Am J Ophthalmol.* 2002;133:135–137.
8. Bayer AU, Ferrari F, Erb C. High occurrence rate of glaucoma among patients with Alzheimer's disease. *Eur Neurol.* 2002; 47:165–168.
9. Tamura H, Kawakami H, Kanamoto T, et al. High frequency of open-angle glaucoma in Japanese patients with Alzheimer's disease. *J Neurol Sci.* 2006;246:79–83.
10. Kesler A, Vakhapova V, Korczyn AD, Naftaliev E, Neudorfer M. Retinal thickness in patients with mild cognitive impairment and Alzheimer's disease. *Clin Neurol Neurosurg.* 2011;113: 523–526.
11. Saccà SC, Centofanti M, Izzotti A. New proteins as vascular biomarkers in primary open angle glaucomatous aqueous humor. *Invest Ophthalmol Vis Sci.* 2012;53:4242–4253.
12. Duan X, Xue P, Wang N, Dong Z, Lu Q, Yang F. Proteomic analysis of aqueous humor from patients with primary open angle glaucoma. *Mol Vis.* 2010;16:2839–2846.
13. Grus FH, Joachim SC, Sandmann S, et al. TTR and complex protein pattern in aqueous humor of patients with primary open-angle glaucoma. *Mol Vis.* 2008;14:1437–1445.
14. Bai Y, Sivori D, Woo SB, Neet KE, Lerner SF, Saragovi HU. During glaucoma, α_2-macroglobulin accumulates in aqueous humor and binds to nerve growth factor, neutralizing neuroprotection. *Invest Ophthalmol Vis Sci.* 2011;52:5260–5265.
15. Tripathi RC, Li J, Chan WF, Tripathi BJ. Aqueous humor in glaucomatous eyes contains an increased level of TGF-2. *Exp Eye Res.* 1994;59:723–727.
16. Tripathi RC, Li J, Tripathi BJ, Chalam KV, Adamis AP. Increased level of vascular endothelial growth factor in aqueous humor of patients with neovascular glaucoma. *Ophthalmology.* 1998; 105:232–237.
17. Welge-Lussen U, May CA, Neubauer AS, Priglinger S. Role of tissue growth factors in aqueous humor homeostasis. *Curr Opin Ophthalmol.* 2001;12:94–99.

18. Hu DN, Ritch R. Hepatocyte growth factor is increased in the aqueous humor of glaucomatous eyes. *J Glaucoma*. 2001;10: 152–157.
19. Wang N, Chintala SK, Fini ME, Schuman JS. Activation of a tissue-specific stress response in the aqueous outflow pathway of the eye defines the glaucoma disease phenotype. *Nat Med*. 2001;7:304–309.
20. Ooi KG, Galatowicz G, Towler HM, Lightman SL, Calder VL. Multiplex cytokine detection versus ELISA for aqueous humor: IL-5, IL-10, and IFNγ profiles in uveitis. *Invest Ophthalmol Vis Sci*. 2006;47:272–277.
21. Wilson MR, Wotherspoon JS. A new microsphere-based immunofluorescence assay using flow cytometry. *J Immunol Methods*. 1988;107:225–230.
22. Vignali DA. Multiplexed particle-based flow cytometric assays. *J Immunol Methods*. 2000;243:243–255.
23. Sharma RK, Rogojina AT, Chalam KV. Multiplex immunoassay analysis of biomarkers in clinically accessible quantities of human aqueous humor. *Mol Vis*. 2009;15:60–69.
24. Kuchtey J, Rezaei KA, Jaru-Ampornpan P, Sternberg PJ, Kuchtey RW. Multiplex cytokine analysis reveals elevated concentration of interleukin-8 in glaucomatous aqueous humor. *Invest Ophthalmol Vis Sci*. 2010;51:6441–6447.
25. Takai Y, Tanito M, Ohira A. Multiplex cytokine analysis of aqueous humor in eyes with primary open-angle glaucoma, exfoliation glaucoma, and cataract. *Invest Ophthalmol Vis Sci*. 2012;53:241–247.
26. Coca-Prados M, Escribano J, Ortego J. Differential gene expression in the human ciliary epithelium. *Prog Retin Eye Res*. 1999;18:403–429.
27. Perrin R, Craig-Schapiro R, Malone J, et al. Identification and validation of novel cerebrospinal fluid biomarkers for staging early Alzheimer's disease. *PLoS One*. 2011;6:e16032.
28. Hu W, Chen-Plotkin A, Arnold S, et al. Novel CSF biomarkers for Alzheimer's disease and mild cognitive impairment. *Acta Neuropathol*. 2010;119:669–678.
29. Craig-Schapiro R, Kuhn M, Xiong C, et al. Multiplexed immunoassay panel identifies novel CSF biomarkers for Alzheimer's disease diagnosis and prognosis. *PLoS One*. 2011;6:e18850.
30. Vickers JC, Craig JE, Stankovich J, et al. The apolipoprotein ε4 gene is associated with elevated risk of normal tension glaucoma. *Mol Vis*. 2002;8:389–393.
31. Copin B, Brézin AP, Valtot F, Dascotte JC, Béchetoille A, Garchon HJ. Apolipoprotein E-promoter single-nucleotide polymorphisms affect the phenotype of primary open-angle glaucoma and demonstrate interaction with the myocilin gene. *Am J Hum Genet*. 2002;70:1575–1581.
32. Abdi F, Quinn JF, Jankovic J, et al. Detection of biomarkers with a multiplex quantitative proteomic platform in cerebrospinal fluid of patients with neurodegenerative disorders. *J Alzheimers Dis*. 2006;9:293–348.
33. Hayashi H, Eguchi Y, Fukuchi-Nakaishi Y, et al. A potential neuroprotective role of apolipoprotein E-containing lipoproteins through low density lipoprotein receptor-related protein 1 in normal tension glaucoma. *J Biol Chem*. 2012;287:25395–25406.
34. Shi Z, Rudzinski M, Meerovitch K, et al. α2-Macroglobulin is a mediator of retinal ganglion cell death in glaucoma. *J Biol Chem*. 2008;283:29156–29165.
35. Bai Y, Dergham P, Nedev H, et al. In chronic and in acute models of retinal neurodegeneration TrkA activity is neuroprotective while p75NTR activity is neurotoxic through a paracrine mechanism. *J Biol Chem*. 2010;285:39392–39400.
36. Hansson S, Andréasson U, Wall M, et al. Reduced levels of amyloid-binding proteins in cerebrospinal fluid from Alzheimer's disease patients. *J Alzheimers Dis*. 2009;16:389–397.
37. Kawaji T, Ando Y, Nakamura M, et al. TTR synthesis in rabbit ciliary pigment epithelium. *Exp Eye Res*. 2005;81:306–312.
38. Kawaji T, Ando Y, Hara R, Tanihara H. Novel therapy for TTR-related ocular amyloidosis: a pilot study of retinal laser photocoagulation. *Ophthalmology*. 2010;117:552–555.
39. Bouhenni RA, Al Shahwan S, Morales J, et al. Identification of differentially expressed proteins in the aqueous humor of primary congenital glaucoma. *Exp Eye Res*. 2011;92:67–75.
40. Saraiva MJ. TTR mutations in hyperthyroxinemia and amyloid diseases. *Hum Mutat*. 2001;17:493–503.
41. Ando Y, Araki S, Ando M. TTR and familial amyloidotic polyneuropathy. *Intern Med*. 1993;32:920–922.
42. Ando Y, Nakamura M, Araki S. TTR-related familial amyloidotic polyneuropathy. *Arch Neurol*. 2005;62:1057–1062.
43. Kimura A, Ando E, Fukushima M, et al. Secondary glaucoma in patients with familial amyloidotic polyneuropathy. *Arch Ophthalmol*. 2003;121:351–356.

Investigative Ophthalmology & Visual Science

別紙４

研究成果の刊行に関する一覧表

研究代表者　京都大学ウイルス研究所　教授　松岡雅雄
研究分担者　熊本大学　教授　尹　浩信

書籍

著者氏名	論文タイトル名	書籍全体の編集者名	書　籍　名	出版社名	出版地	出版年	ページ
尹　浩信	混合性結合組織病	瀧川雅浩、渡辺晋一	皮膚疾患最近の話題2013-2014	南江堂	東京	2013	88
尹　浩信	皮膚科におけるステロイド内服療法。	五十嵐敦之、宮地良樹、清水　宏	一冊で分かる最新皮膚科治療	文光堂	東京	2013	73-75,

雑誌

発表者氏名	論文タイトル名	発表誌名	巻号	ページ	出版年
Yamane K, Jinnin M, Etoh T, Kobayashi Y, Shimozono N, Fukushima S, Masuguchi S, Maruo K, Inoue Y, Ishihara T, Aoi J, Oike Y, Ihn H.	Down-regulation of miR-124/ -214 in cutaneous squamous cell carcinoma mediates abnormal cell proliferation via the induction of ERK.	J Mol Med,	91	69-81	2013
Aoi J, Endo M, Kadomatsu T, Miyata K, Ogata A, Horiguchi H, Odagiri H, Masuda T, Fukushima S, Jinnin M, Hirakawa S, Sawa T, Akaike T, Ihn H, Oike Y.	Angiopoietin-like Protein 2 Accelerates Carcinogenesis by Activating Chronic Inflammation and Oxidative Stress.	Mol Cancer Res,	12	239-49	2014
Ohyoshi Y, Makino T, Nakayama W, Fukushima S, Inoue Y, Jinnin M, Ihn H.	Serum levels of leptin receptor in patients with systemic sclerosis.	Rheumatol Int,			in press.

J Mol Med (2013) 91:69–81
DOI 10.1007/s00109-012-0935-7

ORIGINAL ARTICLE

Down-regulation of miR-124/-214 in cutaneous squamous cell carcinoma mediates abnormal cell proliferation via the induction of ERK

Keitaro Yamane · Masatoshi Jinnin · Tomomi Etoh · Yuki Kobayashi · Naoki Shimozono · Satoshi Fukushima · Shinichi Masuguchi · Keishi Maruo · Yuji Inoue · Tsuyoshi Ishihara · Jun Aoi · Yuichi Oike · Hironobu Ihn

Received: 21 November 2011 / Revised: 10 June 2012 / Accepted: 5 July 2012 / Published online: 25 July 2012

Abstract Squamous cell carcinoma (SCC) is one of the most common skin cancers. Because its potential to recur and metastasize leads to a poor prognosis and significant mortality, it is necessary to develop new early diagnostic tools and new therapeutic approaches. In this study, we found protein levels of ERK1 and ERK2 were increased in SCC cell lines without changing mRNA levels and that ERK1/2 mediates abnormal cell proliferation in these cells. Then, mechanisms underlying the overexpression of ERK1/2 in SCC were investigated focusing on microRNA. We found that miR-214 is the regulator of ERK1, whereas ERK2 is regulated by miR-124 and miR-214. Expression of miR-124 and miR-214 was significantly down-regulated in SCC in vitro and in vivo. Treatment with 5-aza-deoxycytidine and trichostatin A synergistically recovered the miR-124/-214 down-regulation in SCC cell line. However, bisulphite sequencing revealed the methylation status of miR-124/-214 promoter was not increased in the SCC cell line and tumor tissue. Taken together, the down-regulation of miR-124/-214 in SCC is most likely caused, at least in part, by hypermethylation of other promoter regions rather than the miR-124/-214 promoter. Supplementation of these microRNAs in the SCC cell line reduced the abnormal cell proliferation by normalizing ERK1/2 levels. Additionally, serum concentration of miR-124 was correlated with miR-124 expression levels in the tumor tissues and inversely correlated with tumor progression. On the other hand, miR-214 was not detected in the serum. Investigation of the regulatory mechanisms of keratinocyte proliferation by microRNA may lead to develop new biomarkers and treatments using microRNA.

Keywords Cancer · Skin · RNA

K. Yamane · M. Jinnin (✉) · T. Etoh · Y. Kobayashi · N. Shimozono · S. Fukushima · S. Masuguchi · K. Maruo · Y. Inoue · T. Ishihara · J. Aoi · H. Ihn
Department of Dermatology and Plastic Surgery, Faculty of Life Sciences, Kumamoto University, 1-1-1 Honjo, Kumamoto, Japan
e-mail: jinjin1011@hotmail.com

J. Aoi · Y. Oike
Department of Molecular Genetics, Graduate School of Medical Sciences, Kumamoto University, 1-1-1 Honjo, Kumamoto, Japan

Introduction

Basal cell carcinoma, cutaneous squamous cell carcinoma (SCC), and malignant melanoma are the three major types of skin cancer. SCC is a malignant neoplasm of keratinocytes [1]. Although SCC can be seen in many other organs, including the esophagus, urinary bladder, and lungs, cutaneous SCC is characterized by its strong correlation with chronic sun exposure. Most of primary SCCs are considered to be low risk cancers, and are usually treatable, but their potential to recur and metastasize leads to a poor prognosis and significant mortality [2]. Therefore, it is necessary to develop new diagnostic tools for early detection and new therapeutic approaches. However, the pathogenesis of this tumor is still not completely understood.

Recently, several publications revealed tumor cells of SCC have abnormalities in signal transduction pathways. For example, p53, ATF3, TGF-β/Smad, mTORC1, c-Jun

NH(2)-terminal kinase (JNK), fibroblast growth factor receptor 3, and Src have been reported to be involved in the carcinogenesis of SCC [3–10]. In addition, gene mutations in p53 have been found in SCC [11]. Murao et al. also reported that 70 % of SCC show methylation of CpG islands in promoter regions of genes involved in RB1/p16 or p53 pathway [12]. These genetic or epigenetic factors may lead to abnormal cell proliferation seen in SCC.

In this study, we found that ERK protein level was increased in SCC cell lines, and it mediates abnormal cell proliferation in these cells. We then investigated mechanisms underlying the overexpression of ERK in SCC, focusing on microRNA (miRNA). miRNAs, short ribonucleic acid molecules that are only 22 nucleotides long on average, are post-transcriptional regulators that bind to complementary sequences in three prime untranslated regions (3′ UTRs) of mRNAs, leading to gene silencing. Our study demonstrated down-regulation of miR-124 and miR-214 causes the overexpression of ERK in SCC.

Materials and methods

Cell lines

The human cutaneous SCC cell line, DJM-1, was obtained from RIKEN BRC (Tsukuba, Japan). The human pharyngeal SCC cell line, HTB-43, and control Asian keratinocyte cell line, KJB-100, were from ATCC (Manassas, VA) and DS PHARMA (Osaka, Japan), respectively. HaCaT was kindly provided by Dr. Fusenig (German Cancer Research Center, Heidelberg, Germany).

Patient material

Skin specimens were obtained from 20 SCC patients (14 males and 6 females; age range, 58–91 years). Control skin samples were obtained from five patients with seborrheic keratosis (SK). Serum samples were obtained from 32 SCC patients (20 males and 12 females) and 27 healthy volunteers.

Institutional review board approval and written informed consent were obtained according to the Declaration of Helsinki.

Protein array

Panorama Ab Microarray-Cell Signaling kit (Sigma-Aldrich, Deisenhofen, Germany) was used for protein array [13,14]. The complete list of antibodies can be found at Sigma-Aldrich website.

Immunocytochemistry

An immunocytochemical study was performed using anti-p44/42 MAPK (ERK1/2) antibody (Cell Signaling, Beverly, MA) [15].

Western blot analysis

Immunoblotting was performed with an antibody against ERK1/2 or actin (Santa Cruz, CA) [16].

RNA isolation and quantitative real-time polymerase chain reaction

Total RNA was extracted from cultured cells using ISOGEN (Nippon Gene, Tokyo, Japan), or from paraffin-embedded sections with RNeasy FFPE kit (Qiagen, Valencia, CA). cDNA was synthesized from total RNA with PrimeScript RT reagent Kit (Takara Bio Inc, Shiga, Japan). The primer set for GAPDH was purchased from SA Biosciences (Frederick, MD), and the primers for ERK1 or ERK2 were from Takara. DNA was amplified for 40 cycles of denaturation for 15 s at 95 °C and annealing for 30 s at 65 °C.

miRNA isolation from cells or tissues and PCR analysis

miRNA isolation from total RNA was performed using RT^2 qPCR-Grade miRNA Isolation Kit (SA Bioscience). For miRNA polymerase chain reaction (PCR) array, cDNA was mixed with RT^2 SYBR Green/ROX qPCR Master Mix, and the mixture was added into a 96-well RT^2 miRNA PCR Array (SABiosciences). PCR was performed on a Takara Thermal Cycler Dice (TP800)® following the manufacturer's protocol [17].

For quantitative real-time PCR, primers for each miRNA (SABioscience) and template were mixed with SYBR Premix Ex TaqII (Takara Bio Inc). DNA was amplified for 40 cycles of denaturation for 5 s at 95 °C and annealing for 30 s at 60 °C [17].

Isolation and detection of serum miRNAs

miRNA isolation from sera was performed with miRNeasy RNA isolation kit (Qiagen, Valencia, CA), following the manufacturer's instructions with minor modifications [18–20]. To note, 100 μl of serum were supplemented with 5 μl of 5 fmol/μl synthetic non-human miRNA (*Caenorhabditis elegans* miR-39, Takara) as controls providing an internal reference for normalization of technical variations between samples.

For quantitative real-time PCR, primers for each miRNA and templates were mixed with SYBR Advantage qPCR Premix (Takara). DNA was amplified for 40 cycles of denaturation for 5 s at 95 °C and annealing for 20 s at 60 °C.

Table 1 A summary of the up-regulated (>2-fold) proteins in the SCC cell line

Protein	Gene accession number	Fold change
p19INK4d	NP_524145.1	4.93
NAK	NP_037386.1	3.11
Zyxin	NP_035907.1,XP_216124.3,NNP_003452.1	3.05
Protein kinase C (PKC)	NP_036845.2,NP_035232.1,NP_997700.1 NP_036760.1,NP_032881.1,NP_002735.3	2.53
NF-kB	NP_032715.2,NP_003989.2	2.47
Protein kinase Cb2	NP_036845.2	2.39
p300 CBP	NP_064389.2,NP_003875.3,NP_001019423.1	2.22
MAP kinase2 (ERK2)	NP_036079.1,NP_620407.1,NP_446294.1	2.13
Heat shock factor 1	XP_001075095.1,NP_032322.1,NP_005517.1	2.07
MAP1 light chain	NP_955794.1	2.02

Protein array was performed as described in "Materials and methods." The fold change in the expression (the value in DJM-1/the value in KJB-100) was calculated for each protein. Proteins with more than 2-fold difference are shown

Transcript levels of each miRNA were normalized to those of cel-miR-39.

Transient transfection

siRNAs against ERK1 or ERK2 were purchased from Dharmacon (Lafayette, CO). miRNA mimics were from Qiagen. Reverse transfection was performed as described previously [16].

Cell count and BrdU incorporation

Cells were plated at a density of 2×10^4 cells/well in 24-well culture plates. After 72 h, cells were detached from the wells by trypsin treatment and counted using a Coulter® Particle Counter (Beckman Coulter, Fullerton, CA) [16]. The cell proliferation activity was also evaluated by BrdU ELISA kit (Roche, Basel, Switzerland) [21].

Table 2 A summary of the down-regulated (<0.5-fold) proteins in the SCC cell line

Protein	Gene accession number	Fold change
ADAM17	NP_003174.3, NP_033745.4, and NP_064702.1	0.34
TRAIL	NP_003801.1	0.43
Pinin	NP_002678.2, NP_032917.2, and XP_347238.1	0.46
E2F1	NP_005216.1	0.48
Bclx	NP_612815.1, NP_113723.2, and NP_033873.3	0.49

Protein array was performed as described in "Materials and methods". The fold change in the expression (the value in DJM-1/the value in KJB-100) was calculated for each protein. Proteins with more than 2-fold difference are shown

Luciferase reporter assay

The 3′UTR segment of ERK1 or ERK2 was amplified by PCR from human genomic DNA and inserted into pGL3 control vector (Promega Madison, WI) downstream of the stop codon for luciferase. Cells were transfected with luciferase constructs and miRNA mimics by employing Lipofectamine RNAiMAX (Invitrogen, Carlsbad, CA). Renilla luciferase reporter construct was also included in the transfections to correct for variations in the transfection efficiency. The activities of Renilla and firefly luciferases were determined in cell lysates using Dual-Glo Luciferase Assay system (Promega) 48 h after transfection.

Bisulphite sequencing

Genomic DNA was treated with sodium bisulphite using Epitect plus Bisulfite conversion kit (Takara). The methylation status of 5′promoter region of miR-124 and miR-214 was analyzed by bisulfite genomic sequencing. miR-124 promoter region was amplified with following primers: forward, TGAGTGAGAGGATTGTAGTAGGT, reverse, CCTCCATCACTAAATAAAAACAC. And miR-214 promoter region was amplified by: forward, TTTGGAGATTTTGTTTCGTC, reverse, CAACGATCCATAACGTTACTCT. PCR products were subcloned into TOPO TA cloning vector (Invitrogen, San Diego, CA) and sequenced.

Chemical skin carcinogenesis regimen

Skin carcinogenesis was initiated according to a standard 7,12-dimethylbenzanthracene (DMBA)/PMA chemical regimen; 50 μg of DMBA (Sigma-Aldrich) was applied topically to the shaved back skin of 8-week-old female mice (n=6), followed by weekly topical application of 5 μg of the

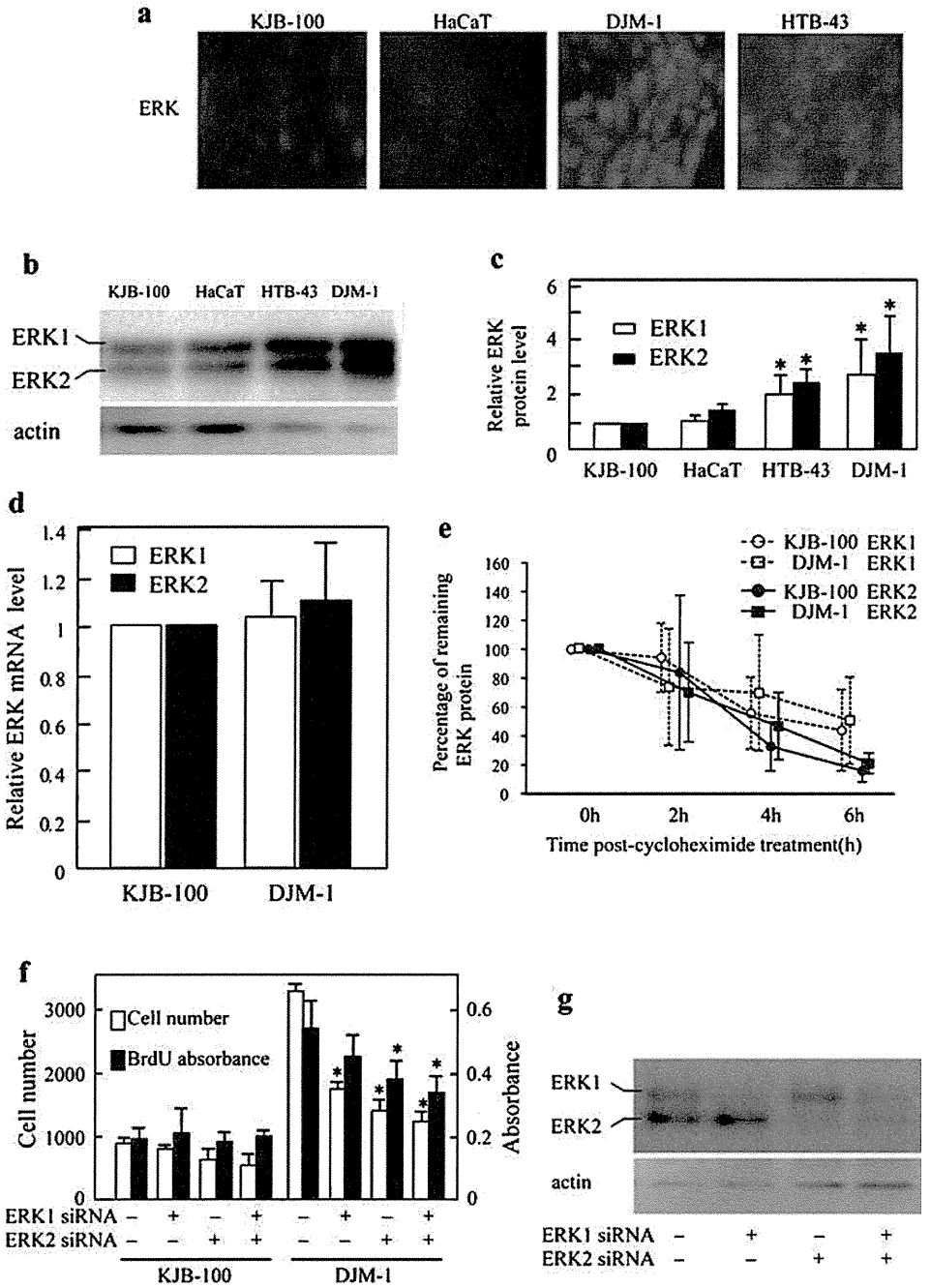

Fig. 1 The expression level and role of ERK in human SCC cell lines and control keratinocyte cell lines. **a** Human control keratinocyte cell lines (KJB-100 and HaCaT) and SCC cell lines (HTB-43 and DJM-1) were stained with an anti-p44/42 MAPK (ERK1/2) antibody. Original magnification, ×40. **b**, **c** Cells were cultured independently until they were confluent. Cell lysates were subjected to immunoblotting with an antibody against ERK1/2. Actin was used as a loading control (**b**). The protein levels of ERK1 (*white bars*) and ERK2 (*black bars*) quantitated by scanning densitometry and corrected for the levels of actin in the same samples are shown relative to those in KJB-100 (1.0). *$P<0.05$, compared with the values in KJB-100 (**c**). **d** KJB-100 and DJM-1 were incubated independently, and their mRNA was purified. A quantitative real-time PCR analysis was performed to determine the mRNA expression levels of ERK1 and ERK2 (normalized to GAPDH). The values in KJB-100 were set at 1. **e** Cell lysates were obtained at the indicated times after cycloheximide treatment. An immunoblot analysis of ERK protein expression was performed. The density of ERK1 (*dotted line*) and ERK2 (*solid lines*) corrected for actin in the same samples was expressed as a percent of the value at time 0 and plotted. **f** KJB-100 and DJM-1 were plated in 24-well plates and transfected with control siRNA, ERK1 siRNA, and/or ERK2 siRNA. After 72 h, the cell numbers were counted by Coulter® Particle Counter (*white bars*). At the same time, cells were labeled with BrdU and analyzed by ELISA (*black bars*). *$P<0.05$ in comparison to the values in DJM-1 transfected with control siRNA. **g** Cells were transfected with control siRNA, ERK1 siRNA, and/or ERK2 siRNA and were incubated for 72 h. Immunoblotting was performed as described in (**b**)

Table 3 A summary of the up-regulated microRNAs in the SCC cell line

Gene name	Fold change	Gene name	Fold change	Gene name	Fold change
let-7g	14.83	miR-16	18.90	miR-29a	13.09
let-7i	9.25	miR-17	50.91	miR-30c	8.22
miR-10a	12.64	miR-18a	28.25	miR-205	8.75
miR-10b	18.38	miR-19a	112.99	miR-301a	14.72
miR-15a	32.22	miR-20a	18.25	miR-378	8.88

microRNAs were purified from KJB-100 and DJM-1, and the microRNA expression profile in each cell type was evaluated using PCR array. The raw threshold cycle (Ct) was normalized using the values of small RNA housekeeping genes. The fold change ($1/2^{\text{the raw Ct of each microRNA–Ct of housekeeping genes}}$) was calculated. microRNAs with more than 8-fold difference (3 Ct difference in ΔΔCT method) are shown

tumor promoter, PMA (Sigma-Aldrich), over 20 weeks as described [22]. This protocol was approved by the Committee on Animal Research at Kumamoto University.

Statistical analysis

Data are expressed as the means±standard deviation of at least three independent experiments. Statistical analysis was carried out with Mann–Whitney test for comparisons of medians. Correlations were assessed by Pearson's correlation coefficient. P values of <0.05 were considered to be significant.

Results

ERK protein expression is up-regulated in human SCC cell lines

As an initial experiment, an antibody microarray was used to identify differences in the expression pattern of various proteins involved in biological functions, including apoptosis and cell cycle regulation, between a control human keratinocyte cell line, KJB-100, and a human cutaneous SCC cell line, DJM-1. Ten among 725 proteins were found to be increased more than 2-fold in DJM-1, while five proteins were down-regulated more than 0.5-fold in the protein array (Tables 1 and 2). Among them, the expression of MAP kinase 2 (ERK2) protein, which is implicated in abnormal cell proliferation of various cancer cells [23–25], was increased by 2.13-fold in DJM-1 compared with that in KJB-100.

To confirm this result, we compared ERK expression between control keratinocytes and SCC cell lines. Immunocytochemical analysis showed increased ERK1/2 expression in DJM-1 and pharyngeal SCC cell line, HTB-43, compared with KJB-100 and HaCaT (another control keratinocyte cell line) (Fig. 1a). By immunoblotting, the protein expression of both ERK1 and ERK2 in DJM-1 and HTB-43 were significantly up-regulated in comparison to that in KJB-100 and HaCaT (Fig. 1b, c). The levels of phosphorylated ERK protein were also

Table 4 A summary of the down-regulated microRNAs in the SCC cell line

Gene name	Fold change	Gene name	Fold change	Gene name	Fold change
let-7a	0.02	miR-127-5p	0.08	miR-193a-5p	0.06
let-7b	0.17	miR-128a	0.09	miR-200c	0.12
let-7f	0.04	miR-132	0.11	miR-203	0.10
miR-1	0.02	miR-133b	0.02	miR-206	0.10
miR-21	0.02	miR-142-5p	0.02	miR-212	0.07
miR-34c-5p	0.07	miR-143	0.13	miR-214	0.08
miR-96	0.02	miR-144	0.02	miR-215	0.05
miR-122	0.03	miR-146a	0.09	miR-218	0.02
miR-124	0.09	miR-150	0.07	miR-372	0.04
miR-125a-5p	0.12	miR-183	0.03	miR-373	0.04
miR-125b	0.06	miR-184	0.04		

microRNAs were purified from KJB-100 and DJM-1, and the microRNA expression profile in each cell type was evaluated using PCR array. The raw threshold cycle (Ct) was normalized using the values of small RNA housekeeping genes. The fold change ($1/2^{\text{the raw Ct of each microRNA–Ct of housekeeping genes}}$) was calculated. microRNAs with more than 8-fold difference (3 Ct difference in ΔΔCT method) are shown

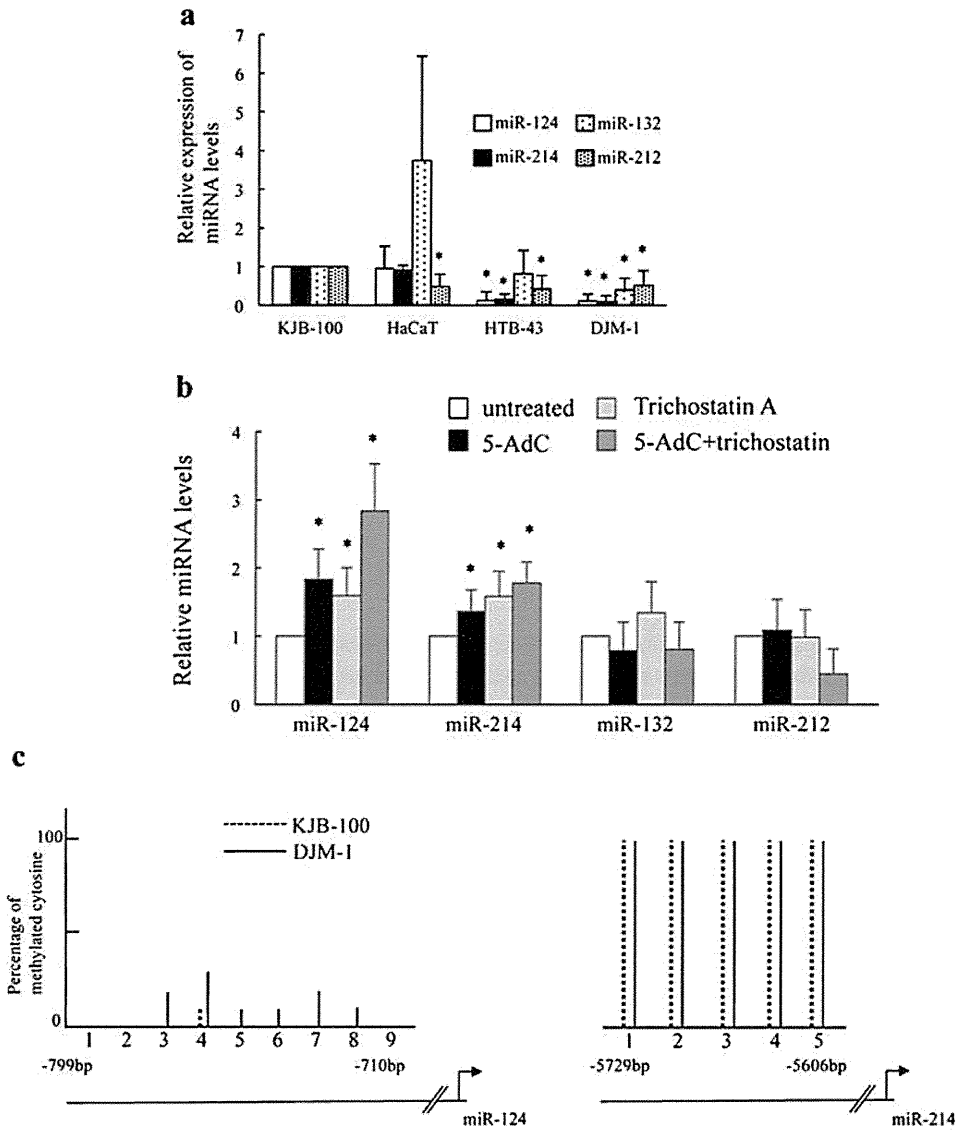

Fig. 2 Expression levels of miR-124 and miR-214 in the human SCC cell line. **a** miRNA was extracted from the indicated cell lines. The relative expression levels of miRNAs were determined by quantitative real-time PCR (normalized to U6). The values in KJB-100 were set at 1. **b** DJM-1 was incubated in the presence or absence of 1 μM 5-AdC and/or 1 μM of trichostatin for 96 h. A quantitative real-time PCR analysis was performed to evaluate the expression levels of miRNAs. *$P<0.05$, compared with the values in untreated cells (1.0, *white bars*). **c** The diagram shows nine CpG sites within the indicated promoter region of miR-124 and five sites within miR-214 promoter. At least five clones were analyzed for methylation status of the promoter region of miR-124 and miR-214 in KJB-100 (*dotted lines*) and DJM-1 (*solid lines*) by bisulfite sequencing in vitro. The methylation status is shown as the percentage of methylated cytosine/number of clones

increased in DJM-1, but the phosphorylation rate (phosphorylated ERK/total ERK) was similar between KJB-100 and DJM-1 (data not shown). Therefore, ERK1/2 was constitutively up-regulated in SCC cell lines. However, the mRNA expression of ERK1 and ERK2 was not altered in DJM-1 compared with KJB-100 (Fig. 1d). In addition, when de novo protein synthesis was blocked by cycloheximide, a protein synthesis inhibitor, decrease ratio of ERK1/2 protein was not different between KJB-100 and DJM-1 (Fig. 1e). Taken together, our results suggested ERK protein expression was likely to be increased in SCC cell lines at the post-transcriptional level.

We then determined whether the increased ERK protein expression contributes to abnormal cellular behaviors of the SCC cell line. DJM-1 has a higher proliferation rate than KJB-100 cells, which was illustrated by increased cell number and BrdU incorporation (Fig. 1f). The knockdown of ERK1 and/or ERK2 by specific siRNAs (Fig. 1g) resulted in the inhibition of such abnormally increased cell number and BrdU incorporation of DJM-1. On the other hand, in KJB-100, the cell number and BrdU incorporation were not significantly affected by the transfection. Thus, the inhibitory effect of these siRNAs on cell proliferation occurred only in DJM-1, indicating that the overexpression of ERK proteins is one of the main pathways mediating the abnormal cell proliferation seen in SCC.

The expression of miR-124 and miR-214 is decreased in SCC cell line

We then asked how ERK protein is down-regulated in DJM-1 without any changes in the mRNA levels. We

hypothesized that miRNA(s) are involved in this process, because miRNAs usually regulate the translation of targets and do not alter mRNA levels. miRNA expression profile in each cell type was evaluated using miRNA PCR array consisting of 88 cancer-related miRNAs (Tables 3 and 4). There were several overexpressed or suppressed miRNAs in DJM-1 compared with KJB-100. Among them, according to miRNA target gene prediction using TargetScan (http://www.targetscan.org/) and Miranda (http://www.microrna.org/microrna/home.do), miR-132, miR-212, or miR-214 are potent regulators of ERK1, and miR-124, miR-132, miR-212, or miR-214 may regulate ERK2. Real-time PCR with specific primers revealed that the levels of miR-124 and miR-214 were decreased in HTB-43 as well as DJM-1 compared with KJB-100 and HaCaT (Fig. 2a). However, miR-132 expression was not decreased in HTB-43 while miR-212 was decreased in HaCaT. Thus, only miR-124 and miR-214 seemed to be specifically decreased in both SCC cell lines.

The treatment of DJM-1 with 5-aza-deoxycytidine (5-AdC), a cytosine analogue refractory to methylation, recovered the down-regulation of both miR-124/-214 slightly (Fig. 2b). Furthermore, trichostatin A, an inhibitor of histone deacetylase, synergistically enhanced the inducible effect of 5-AdC on miR-124/-214 expression, but the expression of miR-132/-212 was not affected by 5-AdC and/or trichostain (Fig. 2b). However, miR-124 promoter and miR-214 promoter was not hypermethylated in DJM-1 compared with KJB-100 by methylation-specific PCR (not shown) or bisulfite sequencing (Fig. 2c): the methylation status of miR-124 promoter was slightly increased in DJM-1 compared with KJB-100 by bisulfite sequencing (Fig. 2c), but there was no significant difference. Similarly, miR-214 promoter was highly methylated both in KJB-100 and DJM-1. Thus, the down-regulation of miR-124/-214 in DJM-1 may be caused by hypermethylation but not by methylation of their promoter regions themselves.

We then determined the correlation of ERK protein expression with miR-124 and miR-214 levels (Table 5). Supplemental expression of miR-124 by the transfection of miRNA mimic into SCC cell lines resulted in the down-regulation of ERK2 protein, but not ERK1 (Fig. 3a), confirming the possibility that ERK2 is the target of miR-124. On the other hand, overexpression of miR-214 mimic resulted in the down-regulation of both ERK1 and ERK2 (Fig. 3b). The transfection of other miRNA mimics specific for miR-132 or miR-212 did not affect ERK1/2 protein expression (Fig. 3c). Thus, the decreased expression of miR-124 and miR-214 may specifically contribute to the overexpression of ERK1/2 proteins in SCC cells.

Table 5 Sequence alignment analysis of the microRNAs and 3′UTR of ERK1 or ERK2

	Position in the 3' UTR	
ERK1 mRNA	466–473	···UUCUGGCUGCCCCAACCUGCUGA···
miR-214		GACGGACAGACACGGACGACA
ERK2 mRNA	3592–3598	···UGCUUUGUACUGUUGGUGCCUUC···
miR-124		CCGUAAGUGGCG--CACGGAAU
ERK2 mRNA	349–356	···UUUUCUACAUGAUGC—CCUGCUGA···
miR-214		GACGGACAGACACGGACGACA
ERK2 mRNA	1168–1174	···CAAAUAUUUCUGAUACUGCUGAG···
miR-214		GACGGACAGACACGGACGACA
ERK2 mRNA	2737–2744	···UGUAAGCAAAAAAUU-CCUGCUGA···
miR-214		GACGGACAGACACGGACGACA

To further determine the direct binding of miRNAs to ERK 3′UTR, we performed a luciferase reporter gene assay. miR-124 mimic reduced only the luciferase activity of ERK1 3′UTR, while miR-214 mimic inhibited the activity of both ERK1 and ERK2 (Fig. 3d). The interdependence of miR-124 and miR-214 were then studied: Simultaneous overexpression of miR-124 and miR-214 further reduced the activity of ERK2 (Fig. 3d), suggesting that the two miRNAs independently mediate ERK2 luciferase activity, and both miRNAs are necessary for the regulation of ERK2. On the other hand, miR-132 and miR-212 did not affect the luciferase activities (Fig. 3e). In addition, the mRNA levels of ERK1 and ERK2 were not affected by miR-124 or miR-214 mimic (Fig. 3f), indicating these miRNAs regulated ERK expression post-transcriptionally.

We then examined the role of miRNAs in the abnormal proliferative activity of keratinocytes via ERK1/2 in SCC. The cell number and BrdU incorporation of DJM-1 were decreased by the transfection of miR-124 or miR-214 mimic (Fig. 3g). miRNA mimic specific for miR-132 or miR-212 did not affect cell proliferation as well as ERK protein expression, as described above. This result supports our hypothesis that the down-regulation of miR-124 and miR-214 induces ERK protein expression and stimulates the proliferation of SCC cells.

ERK protein expression is up-regulated and miR-124/-214 expression is decreased in SCC in vivo

To confirm the in vitro results, we evaluated in vivo expression of ERK and miR-124/-214 in SCC tissues. First, we

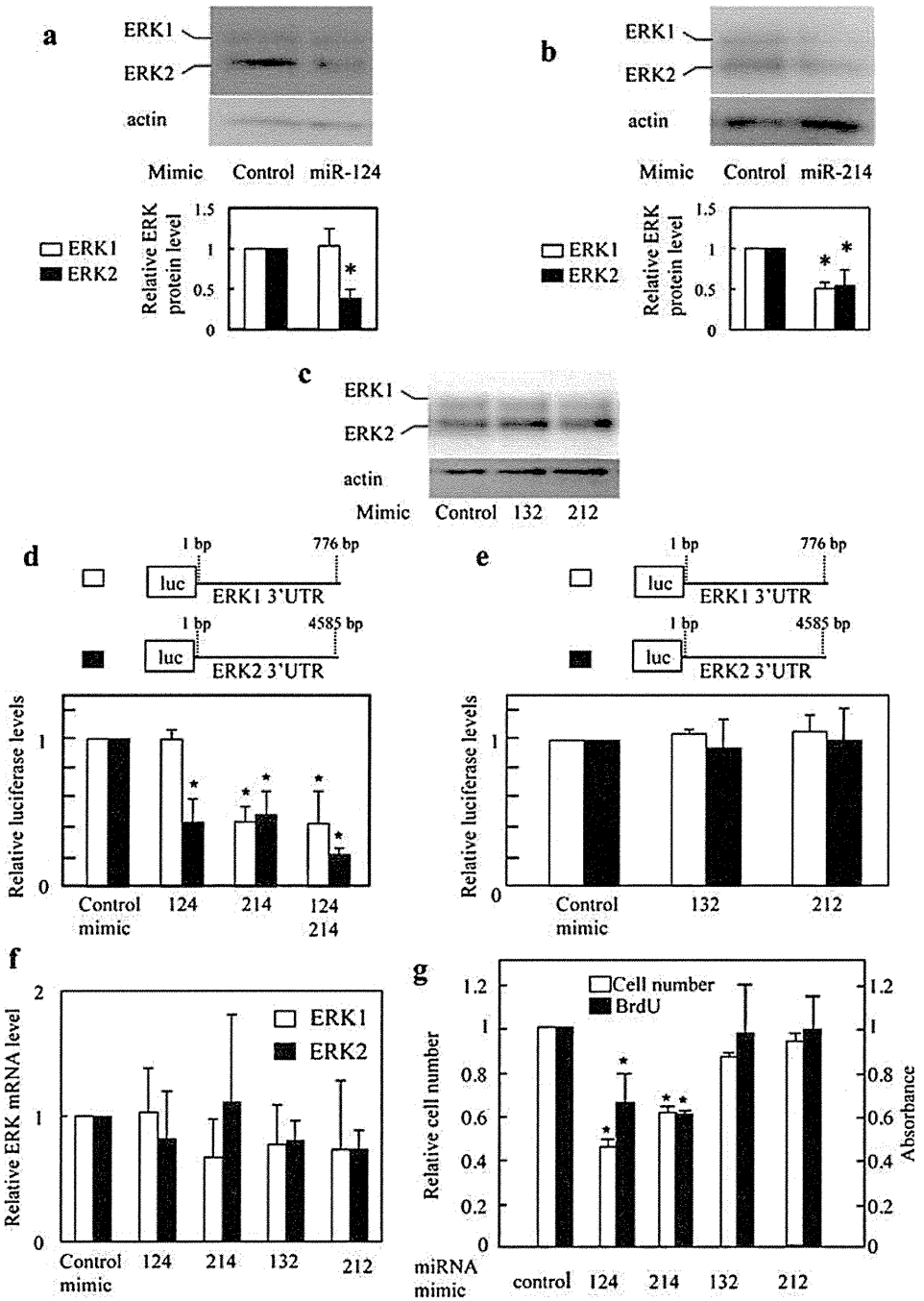

Fig. 3 The regulation of ERK expression by miR-124 and miR-214 in the SCC cell line. **a**, **b** DJM-1 were transfected with miR-124 (**a**) or miR-214 (**b**) mimic. After 72 h, cell lysates were obtained and subjected to immunoblotting to detect ERK and actin. The protein levels of ERK1 (*white bars*) and ERK2 (*black bars*) quantitated by scanning densitometry and corrected for the levels of actin in the same samples are shown relative to those in cells treated with control mimic (1.0). **c** DJM-1 were transfected with miRNA mimics. After 72 h, cell lysates were obtained and subjected to immunoblotting as described in **a**. **d** DJM-1 were transfected with pGL3 luciferase reporter containing 3′ UTR segment of ERK1 (1–776 bp, *white bars*) or ERK2 (1–4,585 bp, *black bars*) and the indicated miRNA mimics. The total amounts of miRNAs were kept constant by adding a control miRNA. The *bar graph* shows the relative luciferase activity; activity in cells treated with control mimic was set at 1. **e** DJM-1 were transfected with pGL3 luciferase reporter containing 3′UTR segment of ERK1 or ERK2 and the indicated miRNA mimics, as described in (**d**). **f** DJM-1 were transfected with the indicated miRNA mimics. The mRNA levels of ERK1 (*white bars*) and ERK2 (*black bars*) were determined by real-time PCR. The values in cells treated with control mimic were set at 1. **g** DJM-1 was transfected with the indicated miRNA mimics. The cell numbers and BrdU incorporation were measured as described in Fig. 1f. *$P<0.05$ in comparison to the values in cells transfected with mimic control (1.0)

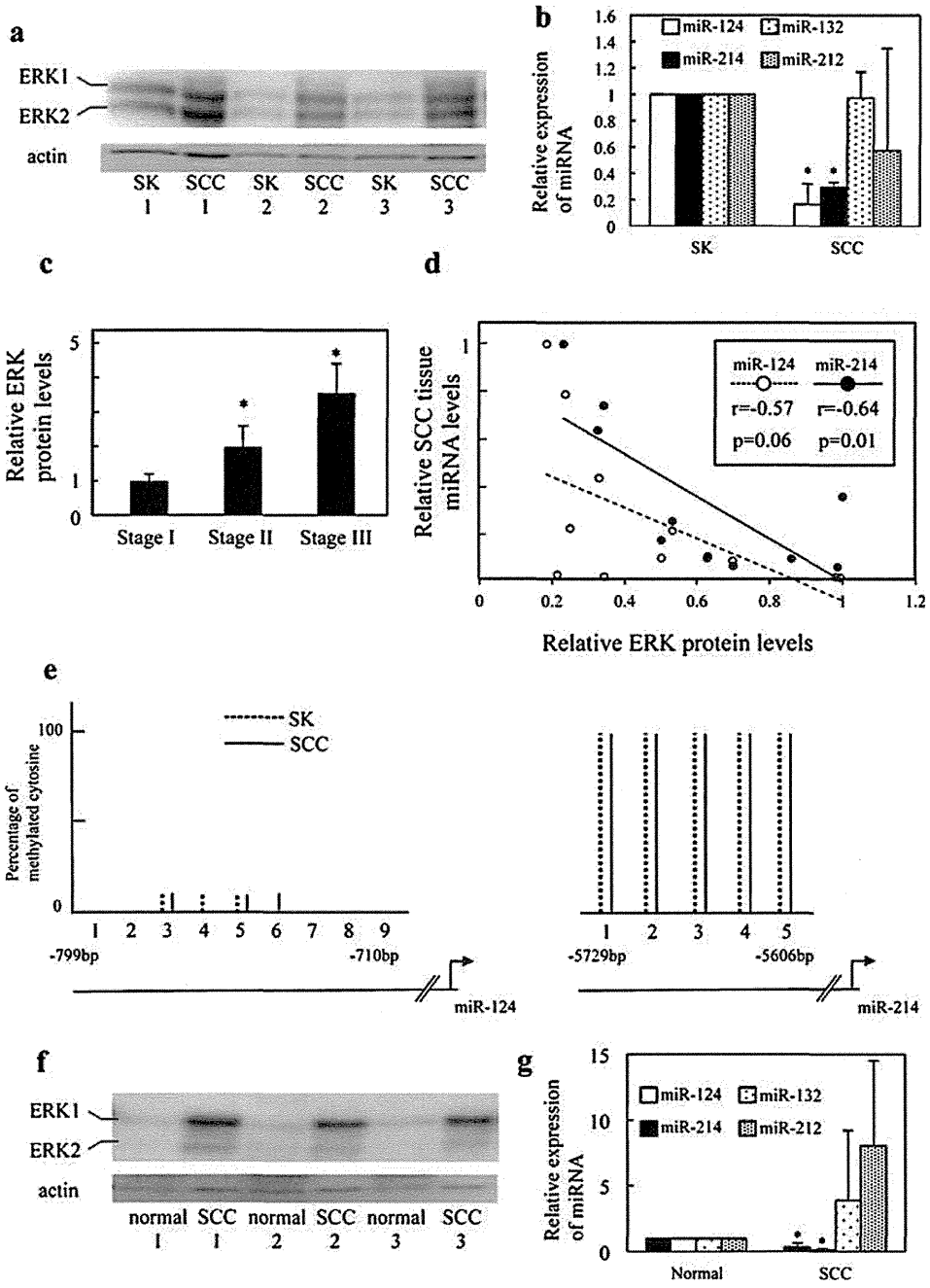

Fig. 4 The expression of ERK1/2, miR-124 and miR-214 in SCC tissues in vivo. **a** Tumor tissues were obtained from patients with SCC or SK. These samples were homogenized and lysed in lysis buffer. Immunoblotting was performed as described in Fig. 1b. Three representative results for five SCC and SK tissue samples are shown. **b** miRNA was purified from three SCC and three SK tissue samples. The relative expression levels of miRNAs were determined by quantitative real-time PCR. *$P<0.05$ in comparison to the values in SK tissues (1.0). **c** The total proteins were extracted from five stage I SCC, five stage II SCC, and three stage III SCC samples. ERK expression was determined by immunoblotting and quantitated as described in Fig. 1c. *$P<0.05$, compared with the values in stage I samples (1.0). **d** The correlation of ERK protein expression (determined by immunoblotting, quantitated by scanning densitometry and corrected for the levels of actin in the same samples) with miR-124 levels (*dotted line*) or miR-214 levels (*solid line*) determined by real-time PCR in each SCC sample. Correlations were assessed by Pearson's correlation coefficient. The maximum value of ERK and miRNA expression levels was set at 1. **e** Methylation status of the promoter region of miR-124 and miR-214 in SK (*dotted lines*) and SCC (*solid lines*) tissues in vivo was determined by bisulfite sequencing as described in Fig. 2c. The methylation status is shown as the percentage of methylated cytosines/number of clones. **f** Normal and SCC tissues were obtained from the same mice. Cell lysates were extracted and subjected to immunoblotting for detection of ERK1/2 protein. Actin was used as a loading control. Three representative results for six SCC and normal tissues are shown. **g** The expression of miRNAs was determined by quantitative real-time PCR using the total miRNA obtained from three normal mouse tissues and three SCC tumor tissues. *$P<0.05$ compared with the values in normal tissues (1.0)

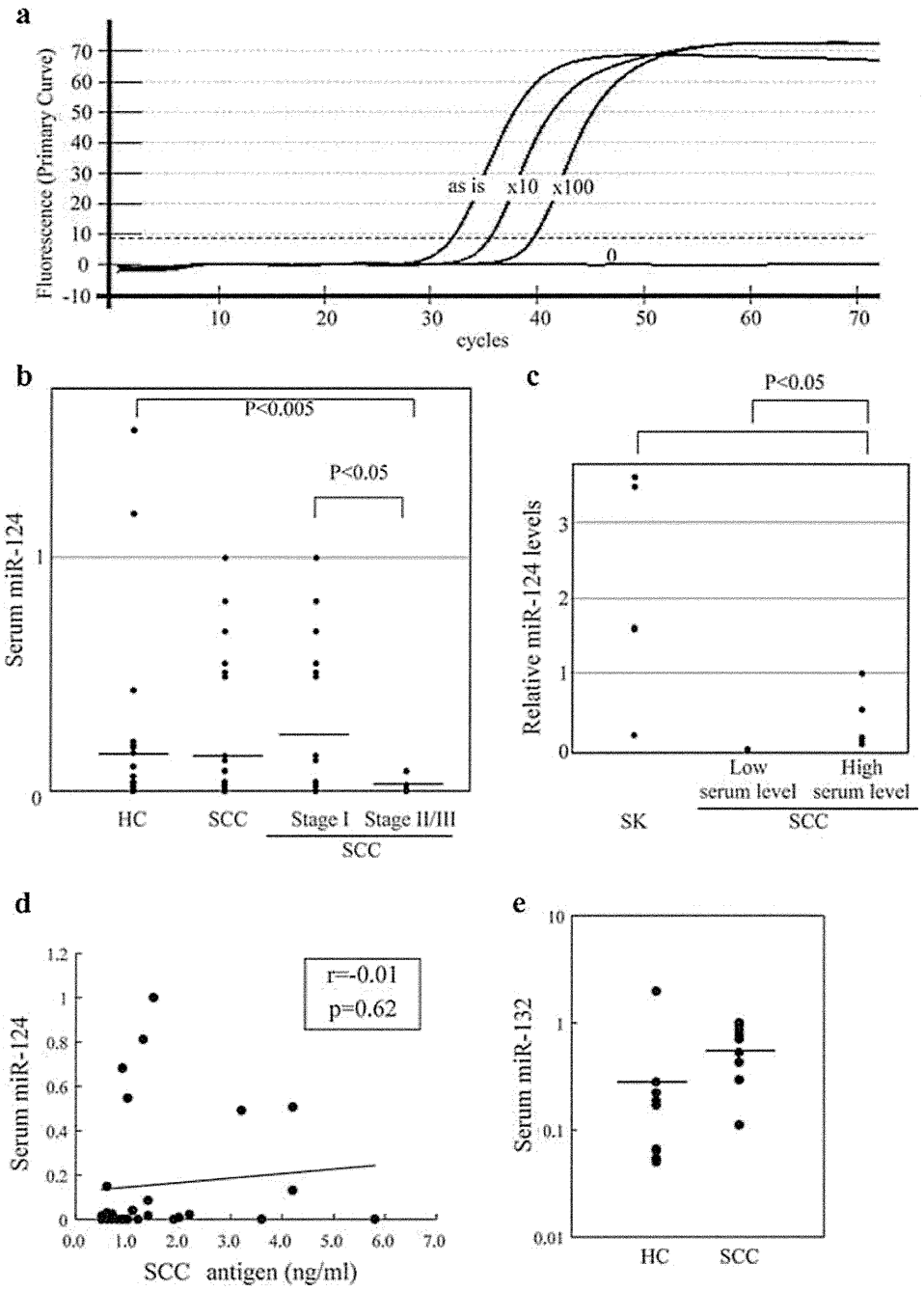

Fig. 5 The serum concentrations of miR-124 in patients with SCC and in healthy control subjects. **a** Serial dilutions of cDNA (as is, 10-fold dilution, 100-fold dilation, or no cDNA added) synthesized from serum miRNA were used as templates for real-time PCR. Amplification curves of gene-specific transcripts are shown to illustrate the exponential increase of fluorescence. The *horizontal dotted line* indicates the threshold. **b** The serum miR-124 levels were measured by real-time PCR. The relative miR-124 concentrations are shown on the ordinate. *Bars* show means. P value was determined using a Mann–Whitney test. *HC* healthy control, *SCC* squamous cell carcinoma. The maximum value in SCC patients was set at 1. **c** Total miRNAs were obtained from tumor tissues of 5 SCC patients with higher serum miR-124 levels, 5 SCC patients with lower miR-124 levels, and 5 SK patients. Relative miR-124 levels in tumor tissues were determined by real-time quantitative PCR as described in "Materials and methods." The maximum value in SCC patients was set at 1. **d** The correlation between serum miR-124 concentration and serum SCC antigen level in each SCC patient. Correlations were assessed by Pearson's correlation coefficient. The maximum value of serum miR-124 level was set at 1. **e** The serum level of miR-132 was determined as described in (**b**). *Bars* show means. *HC* healthy control, *SCC* squamous cell carcinoma. The maximum value in SCC patients was set at 1

compared the protein expression of ERK by immunoblotting using cell lysates obtained from the tumor tissues of SCC and SK, a benign proliferation of keratinocytes (Fig. 4a). ERK1/2 protein level was increased in SCC tissues compared with SK tissues, consistent with the in vitro results. Also, as expected, the expression of both miR-124 and miR-214 was significantly decreased in SCC, but miR-132 was not (Fig. 4b). miR-212 expression tended to be decreased in SCC tissue, but it was not significant due to high variation between samples. In addition, ERK protein levels were increased in samples from a higher stage of SCC (Fig. 4c). The miR-214 levels were significantly and inversely correlated with ERK protein expression in the same tissues ($r=-0.64$; $p=-0.01$, Fig. 4d). In addition, although not statistically significant, miR-124 also tended to be inversely correlated with ERK expression ($r=-0.57$; $p=0.06$). Consistent with the in vitro results, in vivo methylation status of the promoter regions of miR-124/-214 did not show any significant differences between SK and SCC samples (Fig. 4e). To further confirm these results, we next

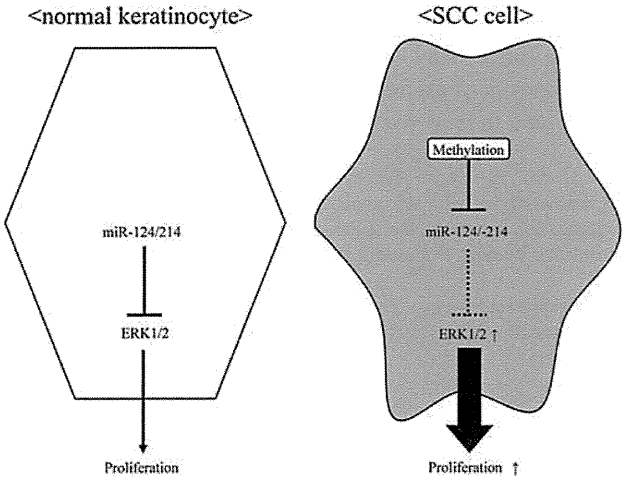

Fig. 6 A schematic representation of the miR-124/-214-ERK1/2 cascade in SCC tumor cells. In SCC keratinocytes, the down-regulation of miR-124/-214 in SCC is most likely caused, at least in part, by hypermethylation of other promoter regions rather than the miR-124/-214 promoter. The decreased miR-124/-214 expression results in up-regulation of ERK1/2 protein expression without altering the mRNA levels. The increased ERK1/2 mediates the hyperproliferation of SCC tumor cells

determined the expression of ERK and miRNAs in a mouse SCC model treated with DMBA and PMA [22]. When SCC tissues were compared with normal tissues from the same mice, ERK1/2 overexpression and miR-124/-214 down-regulation were observed in SCC tissues (Fig. 4f, g). Taken together, miR-124/-214-ERK1/2 pathway may play an important role in the pathogenesis of SCC both in vitro and in vivo.

The serum concentration of miR-124 is decreased in SCC patients

Finally, we determined the serum concentrations of miR-124/-214 and evaluated the possibility that serum levels of these miRNAs can be a disease marker for SCC.

There have been no previous reports demonstrating the expression of miR-124/-214 in cell-free body fluid. To validate that these miRNAs are indeed detectable in human serum, miRNAs were extracted from the sera of healthy individuals and the levels of miR-124 or miR-214 were determined by quantitative real-time PCR [18–20,26] (Fig. 5a). miR-214 was not detected in the serum, while the amplification of miR-124 was observed, and Ct values were increased by serial dilution of the miRNA. Thus, miR-124, but not miR-214, was thought to be detectable and quantifiable in the serum using our method.

Serum samples were obtained from 32 patients with cutaneous SCC (stage I~III). Twenty-seven healthy control subjects were also included in this study. As shown in Fig. 5b, serum miR-124 levels in SCC patients were lower than those in healthy controls, but not significant ($p=0.11$). However, when these SCC patients were grouped according to TNM classification system (21 stage I patients, 8 stage II patients, and 3 stage III patients), the stage II/III patients showed a significantly lower miR-124 concentration compared with healthy controls ($p<0.005$) and stage I patients ($p<0.05$). Notably, the miR-124 levels of all 11 patients with stage II/III SCC were almost the same as the background levels. This result suggested that serum miR-124 level might be a new tumor marker for SCC. Furthermore, as shown in Fig. 5c, miR-124 expression in tumor tissues from SCC patients with lower serum miR-124 levels were significantly decreased in comparison to those with higher serum levels, suggesting that serum miR-124 levels reflect miR-124 expression in the tumor tissue. miR-124 levels in tumor tissues from SCC patients with higher serum miR-124 levels were still significantly lower than those in SK patients. On the other hand, serum SCC antigen was elevated (>1.5 ng/ml) in only 9 out of 32 patients (five stage I patients and four stage II/III patients). The serum miR-124 level was not correlated with the serum levels of SCC antigen ($r=-0.01$, $p=0.52$; Fig. 5d).

Serum miR-132 levels were not significantly different between healthy controls and SCC patients (Fig. 5e) while miR-212 was not detected in the serum.

Discussion

In this study, we have presented three major findings. First, we found ERK1/2 protein to be overexpressed in SCC post-transcriptionally. This ERK overexpression may be responsible for the abnormal cell proliferation in SCC. A protein array analysis showed ERK2 protein expression was increased in SCC by more than 2-fold while ERK1 not. Because the array analysis was performed as a single experiment, a statistical significance could not be evaluated. Therefore, we confirmed the result using a different method, accompanied by statistical analysis: immunoblotting showed both ERK1 and ERK2 were significantly up-regulated in SCC cell lines. The overexpression of ERK has been reported in many types of cancers, including oral SCC [25]. In addition, the most recent studies indicate that one of the adverse effects of BRAF inhibitor vemurafenib, a new agent against malignant melanoma, is the development of cutaneous SCC, and such SCC may be caused by the transactivation of downstream ERK signaling [27,28]. Thus, it is important to clarify the association between ERK signaling and the pathogenesis of SCC.

Second, we found that the expression of miR-124 and miR-214 was down-regulated in SCC both in vitro and in vivo, and that supplementation of these miRNAs in DJM-1 normalized its abnormal cell proliferation via the down-regulation of ERK. In breast cancer, miR-17-5p was reported to cause carcinogenesis by altering the expression of HMG box-containing protein 1 [29]. Our results suggest that miRNAs are also involved in the pathogenesis of cutaneous SCC.

Third, we investigated serum miRNA levels in SCC patients. Increasing evidence has recently shown that serum miRNAs can be used as biomarkers, especially for various malignant tumors [30,31]. For example, serum miR-221 level is increased in melanoma patients, and elevation of serum miR-221 level is useful for predicting the presence of a tumor [26]. In our study, the serum concentration of miR-124 was significantly decreased in patients with stage II/III SCC. To date, although SCC antigen is a known tumor marker for SCC, the serum levels of SCC antigen usually remain within normal limits in patients with smaller-sized, nonmetastatic SCC or SCC in situ, while they are significantly elevated in patients with large, invasive, or metastatic SCC [32]. Thus, the identification of another tumor marker sensitive for early stage SCC is urgently needed for early diagnosis. Our results indicate serum miR-124 level may be more sensitive biomarker of the tumor than SCC antigen, because all of the eight stage II SCC patients and three stage III patients in our study showed low serum miR-124 levels while only two of the eight stage II patients and two of the three stage III patients had elevated SCC antigen levels.

Numerous studies have suggested not only up-regulated but also down-regulated circulating miRNAs can be used to discriminate patients with various cancers from healthy controls [33]: for example, miR-24 in prostate cancer or let-7f, miR-20b, and miR-30e-3p in nonsmall cell lung cancer [34,35]. Although the mechanism by which a localized tumor can decrease the serum miRNA level is still unknown, we hypothesized systemic hypermethylation of the miRNA loci can cause such decrease. Our study using 5-AdC and trichostatin A revealed the down-regulation of miR-124 is caused, at least partly, by hypermethylation. However, the promoter of miR-124 in the SCC cell line was not hypermethylated in comparison to controls. Therefore, the miR-124 level in SCC is most likely controlled by hypermethylation of other promoter regions (e.g., genes in the RB1/p16 or p53 pathway, as described in "Introduction") rather than the miR-124/-214 promoter, and the low serum miR-124 level in SCC patients may be caused by systemic hypermethylation (e.g., due to systemic sun exposure).

Taken together, a hypothetical model of the hyperproliferation seen in SCC tumor cells was provided by our results as shown in Fig. 6. Further investigation of the regulatory mechanism(s) underlying the abnormal keratinocyte proliferation induced by miRNAs in the skin may lead to the development of useful biomarkers for early detection of this tumor and to new treatments using miRNA.

Acknowledgments We thank Ms. Junko Suzuki and Ms. Chiemi Shiotsu for their valuable technical assistance. We also would like to thank Dr. Norbert E. Fusenig for kindly providing HaCaT.

Disclosure statement The authors declare that they have no competing financial interests that might influence the results and discussion in this paper.

References

1. Alam M, Ratner D (2001) Cutaneous squamous-cell carcinoma. N Engl J Med 344:975–983
2. Pfaff D, Philippova M, Buechner S, Maslova K, Mathys T, Erne P, Resink T (2010) T-cadherin loss induces an invasive phenotype in human keratinocytes and squamous cell carcinoma (SCC) cells in vitro and is associated with malignant transformation of cutaneous SCC in vivo. Br J Dermatol 163:353–363
3. Wu X, Nguyen B, Dziunycz P, Chang S, Brooks Y, Lefort K, Hofbauer G, Dotto G (2010) Opposing roles for calcineurin and ATF3 in squamous skin cancer. Nature 465:368–372
4. Ganapathy A, Paterson IC, Prime SS, Eveson JW, Pring M, Price N, Threadgold SP, Davies M (2010) TGF-β inhibits metastasis in late stage human squamous cell carcinoma of the skin by a mechanism that does not involve Id1. Cancer Lett 298:107–118
5. Kubo M, Ihn H, Yamane K, Asano Y, Jinnin M, Tamaki K (2001) Differential expression of transforming growth factor-beta receptors in squamous cell carcinoma. Br J Dermatol 145:840–842
6. Lu ZH, Shvartsman MB, Lee AY, Shao JM, Murray MM, Kladney RD, Fan D, Krajewski S, Chiang GG, Mills GB et al (2010) Mammalian target of rapamycin activator RHEB is frequently overexpressed in human carcinomas and is critical and sufficient for skin epithelial carcinogenesis. Cancer Res 70:3287–3298
7. Ke H, Harris R, Coloff JL, Jin JY, Leshin B, Miliani de Marval P, Tao S, Rathmell JC, Hall RP, Zhang JY (2010) The c-Jun NH2-terminal kinase 2 plays a dominant role in human epidermal neoplasia. Cancer Res 70:3080–3088
8. Hida Y, Kubo Y, Arase S (2009) Activation of fibroblast growth factor receptor 3 and oncogene-induced senescence in skin tumours. Br J Dermatol 160:1258–1263
9. Ayli EE, Li W, Brown TT, Witkiewicz A, Elenitsas R, Seykora JT (2008) Activation of Src-family tyrosine kinases in hyperproliferative epidermal disorders. J Cutan Pathol 35:273–277
10. Zhao L, Li W, Marshall C, Griffin T, Hanson M, Hick R, Dentchev T, Williams E, Werth A, Miller C et al (2009) Srcasm inhibits Fyn-induced cutaneous carcinogenesis with modulation of Notch1 and p53. Cancer Res 69:9439–9447
11. Kubo Y, Urano Y, Yoshimoto K, Iwahana H, Fukuhara K, Arase S, Itakura M (1994) p53 gene mutations in human skin cancers and precancerous lesions: comparison with immunohistochemical analysis. J Investig Dermatol 102:440–444
12. Murao K, Kubo Y, Ohtani N, Hara E, Arase S (2006) Epigenetic abnormalities in cutaneous squamous cell carcinomas: frequent inactivation of the RB1/p16 and p53 pathways. Br J Dermatol 155:999–1005
13. Smith L, Watson M, O'Kane S, Drew P, Lind M, Cawkwell L (2006) The analysis of doxorubicin resistance in human breast

cancer cells using antibody microarrays. Mol Cancer Ther 5:2115–2120
14. Kopf E, Shnitzer D, Zharhary D (2005) Panorama Ab Microarray Cell Signaling kit: a unique tool for protein expression analysis. Proteomics 5:2412–2416
15. Moriya C, Jinnin M, Yamane K, Maruo K, Muchemwa FC, Igata T, Makino T, Fukushima S, Ihn H (2011) Expression of matrix metalloproteinase-13 is controlled by IL-13 via PI3K/Akt3 and PKC-δ in normal human dermal fibroblasts. J Investig Dermatol 131:655–661
16. Makino T, Jinnin M, Muchemwa FC, Fukushima S, Kogushi-Nishi H, Moriya C, Igata T, Fujisawa A, Johno T, Ihn H (2010) Basic fibroblast growth factor stimulates the proliferation of human dermal fibroblasts via the ERK1/2 and JNK pathways. Br J Dermatol 162:717–723
17. Nakashima T, Jinnin M, Etoh T, Fukushima S, Masuguchi S, Maruo K, Inoue Y, Ishihara T, Ihn H (2010) Down-regulation of mir-424 contributes to the abnormal angiogenesis via MEK1 and cyclin E1 in senile hemangioma: its implications to therapy. PLoS One 5:e14334
18. Kroh EM, Parkin RK, Mitchell PS, Tewari M (2010) Analysis of circulating microRNA biomarkers in plasma and serum using quantitative reverse transcription-PCR (qRT-PCR). Methods 50:298–301
19. Gilad S, Meiri E, Yogev Y, Benjamin S, Lebanony D, Yerushalmi N, Benjamin H, Kushnir M, Cholakh H, Melamed N et al (2008) Serum microRNAs are promising novel biomarkers. PLoS One 3: e3148
20. Mitchell PS, Parkin RK, Kroh EM, Fritz BR, Wyman SK, Pogosova-Agadjanyan EL, Peterson A, Noteboom J, O'Briant KC, Allen A et al (2008) Circulating microRNAs as stable blood-based markers for cancer detection. Proc Natl Acad Sci U S A 105:10513–10518
21. Jinnin M, Medici D, Park L, Limaye N, Liu Y, Boscolo E, Bischoff J, Vikkula M, Boye E, Olsen BR (2008) Suppressed NFAT-dependent VEGFR1 expression and constitutive VEGFR2 signaling in infantile hemangioma. Nat Med 14:1236–1246
22. Hirakawa S, Kodama S, Kunstfeld R, Kajiya K, Brown LF, Detmar M (2005) VEGF-A induces tumor and sentinel lymph node lymphangiogenesis and promotes lymphatic metastasis. J Exp Med 201:1089–1099
23. Handra-Luca A, Bilal H, Bertrand JC, Fouret P (2003) Extracellular signal-regulated ERK-1/ERK-2 pathway activation in human salivary gland mucoepidermoid carcinoma: association to aggressive tumor behavior and tumor cell proliferation. Am J Pathol 163:957–967
24. Steinmetz R, Wagoner HA, Zeng P, Hammond JR, Hannon TS, Meyers JL, Pescovitz OH (2004) Mechanisms regulating the constitutive activation of the extracellular signal-regulated kinase (ERK) signaling pathway in ovarian cancer and the effect of ribonucleic acid interference for ERK1/2 on cancer cell proliferation. Mol Endocrinol 18:2570–2582
25. Mishima K, Inoue K, Hayashi Y (2002) Overexpression of extracellular-signal regulated kinases on oral squamous cell carcinoma. Oral Oncol 38:468–474
26. Kanemaru H, Fukushima S, Yamashita J, Honda N, Oyama R, Kakimoto A, Masuguchi S, Ishihara T, Inoue Y, Jinnin M et al (2011) The circulating microRNA-221 level in patients with malignant melanoma as a new tumor marker. J Dermatol Sci 61:187–193
27. Poulikakos PI, Zhang C, Bollag G, Shokat KM, Rosen N (2010) RAF inhibitors transactivate RAF dimers and ERK signalling in cells with wild-type BRAF. Nature 464:427–430
28. Hatzivassiliou G, Song K, Yen I, Brandhuber BJ, Anderson DJ, Alvarado R, Ludlam MJ, Stokoe D, Gloor SL, Vigers G et al (2010) RAF inhibitors prime wild-type RAF to activate the MAPK pathway and enhance growth. Nature 464:431–435
29. Li H, Bian C, Liao L, Li J, Zhao R (2010) miR-17-5p promotes human breast cancer cell migration and invasion through suppression of HBP1. Breast Cancer Res Treat 126:565–575
30. Gaur A, Jewell DA, Liang Y, Ridzon D, Moore JH, Chen C, Ambros VR, Israel MA (2007) Characterization of microRNA expression levels and their biological correlates in human cancer cell lines. Cancer Res 67:2456–2468
31. Cortez MA, Calin GA (2009) MicroRNA identification in plasma and serum: a new tool to diagnose and monitor diseases. Expert Opin Biol Ther 9:703–711
32. Yagi H, Danno K, Maruguchi Y, Yamamoto M, Imamura S (1987) Significance of squamous cell carcinoma (SCC)-related antigens in cutaneous SCC. A preliminary report. Arch Dermatol 123:902–906
33. Zhao H, Shen J, Medico L, Wang D, Ambrosone CB, Liu S (2010) A pilot study of circulating miRNAs as potential biomarkers of early stage breast cancer. PLoS One 5:e13735
34. Moltzahn F, Olshen AB, Baehner L, Peek A, Fong L, Stöppler H, Simko J, Hilton JF, Carroll P, Blelloch R (2011) Microfluidic-based multiplex qRT-PCR identifies diagnostic and prognostic microRNA signatures in the sera of prostate cancer patients. Cancer Res 71:550–560
35. Silva J, García V, Zaballos A, Provencio M, Lombardía L, Almonacid L, García JM, Domínguez G, Peña C, Diaz R et al (2011) Vesicle-related microRNAs in plasma of nonsmall cell lung cancer patients and correlation with survival. Eur Respir J 37:617–623

Published OnlineFirst November 20, 2013; DOI: 10.1158/1541-7786.MCR-13-0336

Molecular Cancer Research

DNA Damage and Repair

Angiopoietin-like Protein 2 Accelerates Carcinogenesis by Activating Chronic Inflammation and Oxidative Stress

Jun Aoi[1,2], Motoyoshi Endo[1], Tsuyoshi Kadomatsu[1], Keishi Miyata[1], Aki Ogata[1,2], Haruki Horiguchi[1], Haruki Odagiri[1], Tetsuro Masuda[1], Satoshi Fukushima[2], Masatoshi Jinnin[2], Satoshi Hirakawa[3], Tomohiro Sawa[4,5], Takaaki Akaike[4], Hironobu Ihn[2], and Yuichi Oike[1,6]

Abstract

Chronic inflammation has received much attention as a risk factor for carcinogenesis. We recently reported that Angiopoietin-like protein 2 (Angptl2) facilitates inflammatory carcinogenesis and metastasis in a chemically induced squamous cell carcinoma (SCC) of the skin mouse model. In particular, we demonstrated that Angptl2-induced inflammation enhanced susceptibility of skin tissues to "preneoplastic change" and "malignant conversion" in SCC development; however, mechanisms underlying this activity remain unclear. Using this model, we now report that transgenic mice overexpressing Angptl2 in skin epithelial cells (K14-*Angptl2* Tg mice) show enhanced oxidative stress in these tissues. Conversely, in the context of this model, *Angptl2* knockout (KO) mice show significantly decreased oxidative stress in skin tissue as well as a lower incidence of SCC compared with wild-type mice. In the chemically induced SCC model, treatment of K14-*Angptl2* Tg mice with the antioxidant *N*-acetyl cysteine (NAC) significantly reduced oxidative stress in skin tissue and the frequency of SCC development. Interestingly, K14-*Angptl2* Tg mice in the model also showed significantly decreased expression of mRNA encoding the DNA mismatch repair enzyme Msh2 compared with wild-type mice and increased methylation of the *Msh2* promoter in skin tissues. *Msh2* expression in skin tissues of Tg mice was significantly increased by NAC treatment, as was *Msh2* promoter demethylation. Overall, this study strongly suggests that the inflammatory mediator Angptl2 accelerates chemically induced carcinogenesis through increased oxidative stress and decreased *Msh2* expression in skin tissue.

Implications: Angptl2-induced inflammation increases susceptibility to microenvironmental changes, allowing increased oxidative stress and decreased Msh2 expression; therefore, Angptl2 might be a target to develop new strategies to antagonize these activities in premalignant tissue. *Mol Cancer Res; 12(2); 1–11. ©2013 AACR.*

Introduction

The connection between cancer and inflammation was first made in the 19th century (1). Since then, epidemiologic studies have confirmed the idea that chronic inflammation underlies many cancers (2). Recently, we reported that Angiopoietin-like protein 2 (Angptl2) acts as a chronic inflammatory mediator in several pathologic settings (3–6), and demonstrated that increased Angptl2 expression in skin tissues promotes inflammation and accelerates carcinogenesis in a chemically induced squamous cell carcinoma (SCC) of the skin mouse model by increasing susceptibility to "preneoplastic change" and "malignant conversion" (7). In normal cells, initiating oncogenic mutation is considered essential to promote a "preneoplastic change," which, if unrepaired, is then followed by proliferation and acquisition of cellular survival capacity, allowing accumulation of additional mutations (8–10). Potentially oncogenic mutations can be antagonized by DNA repair mechanisms, some mediated by members of the mismatch repair (MMR) family, which corrects base mispairings or repairs larger insertion/deletion loops (IDL; refs 11–14). In the MMR system, three homologs of the bacterial MutS protein—Msh2, Msh3, and Msh6—form heterodimers that recognize DNA damage (15). Loss-of-function mutations or epigenetic silencing of MMR genes increase genomic microsatellite instability (MSI), increasing the rate of DNA replication errors (16). Genetic and biochemical studies indicate that Msh2 is a critical component of all MMR complexes and, consequently, *Msh2*-null mutants are predicted to completely the lack

Authors' Affiliations: Departments of [1]Molecular Genetics and [2]Dermatology and Plastic Surgery, Graduate School of Medical Sciences, Kumamoto University, Kumamoto; [3]Department of Dermatology, Hamamatsu University School of Medicine, Hamamatsu; [4]Department of Environmental Health Sciences and Molecular Toxicology, Tohoku University Graduate School of Medicine, Sendai; [5]PRESTO, Japan Science and Technology Agency, Kawaguchi, Saitama, Japan; and [6]Core Research for Evolutional Science and Technology (CREST), Japan Science and Technology Agency, Tokyo, Japan

Note: Supplementary data for this article are available at Molecular Cancer Research Online (http://mcr.aacrjournals.org/).

Corresponding Authors: Yuichi Oike, Department of Molecular Genetics, Graduate School of Medical Sciences, Kumamoto University, 1-1-1 Honjo, Kumamoto 860-8556, Japan. Phone: 81-96-373-5142; Fax: 81-96-373-5145; E-mail: oike@gpo.kumamoto-u.ac.jp; and Motoyoshi Endo, E-mail: enmoto@gpo.kumamoto-u.ac.jp

doi: 10.1158/1541-7786.MCR-13-0336

Published OnlineFirst November 20, 2013; DOI: 10.1158/1541-7786.MCR-13-0336

MMR response (17, 18). Significantly, loss or mutation of mammalian *Msh2* increases the probability of developing certain types of tumors (19).

In this study, we report that K14-*Angptl2* Tg mice, which show accelerated skin tissue inflammation and greater frequency of chemically induced SCC, showed enhanced oxidative stress in skin tissues and decreased expression of *Msh2*, likely due to increased methylation of the *Msh2* promoter. Interestingly, treatment of these mice with the antioxidant *N*-acetyl cysteine (NAC) significantly reduced oxidative stress in skin tissue and SCC frequency. Furthermore, *Msh2* mRNA expression in skin tissue of Tg mice significantly increased following NAC treatment in parallel with demethylation of the *Msh2* promoter region. Overall, these findings suggest that Angptl2-induced inflammation increases susceptibility to microenvironmental changes allowing accumulation of oncogenic DNA mutations.

Materials and Methods

Mice

Male mice were used for the experiments. Mice were housed in a temperature-controlled room with a 12-hour light/dark cycle. Food and water were available *ad libitum* unless otherwise noted. Mice were fed a normal diet (CE-2; CLEA, Japan). For some experiments, NAC (40 mmol/L) was administered in drinking water from 7 weeks after birth until the end of the experiments. For chemical carcinogenesis assays, K14-*Angptl2* Tg (3) and *Angptl2* KO (3) were backcrossed to the FVB/N strain for more than 10 generations. During the course of the experiment, we observed no significant difference in body weight between K14-*Angptl2* Tg and wild-type littermate mice or between *Angptl2* KO and wild-type littermates. In addition, we observed no significant difference in body weight between these groups, with or without NAC treatment. All experiments were performed according to the guidelines of the Institutional Animal Committee of Kumamoto University.

Chemically induced skin carcinogenesis

We performed chemical skin carcinogenesis experiments using K14-*Angptl2* Tg mice, *Angptl2* KO mice, and respective wild-type littermates as controls, as described previously (20, 21). Briefly, 50 μg of the chemical initiator mutagen 7,12-dimethylbenzanthracene (DMBA; Sigma) was applied topically to the shaved skin on the back of 8-week-old male mice, followed by weekly topical application of 5 μg of the tumor promoter phorbol ester 12-O-tetradecanoylphorbol 13-acetate (PMA; Sigma) over 20 weeks. Raised lesions of a minimum diameter of 1 mm present for at least 1 week were scored as papillomas. Large papillomas were defined as papillomas of 3 mm or more in diameter. Mice were killed after 45 weeks or at 8 weeks after the first diagnosis of SCC. SCC evaluation was carried out clinically and histologically by two independent dermatologists using specified standards (20–22). Clinically, SCCs are significantly larger and grow more rapidly than papillomas. Histologically, papillomas show loss of polarity and anaplasia of the nuclei localized to the epidermis. However, SCCs are invasive carcinomas of the surface epidermis. SCCs proliferate downward into the dermis. The ratio of malignant conversion was calculated for each group of mice as the total number of SCC divided by the number of large papillomas and expressed as a percentage. The two-sided unpaired Student *t*-test was used to analyze differences in the number of tumors per mice with or without NAC treatment.

Immunoblot analysis

Skin tissues were homogenized in lysis buffer (10 mmol/L NaF, 1 mmol/L Na_3VO_4, 1 mmol/L EDTA, 300 mmol/L NaCl, 50 mmol/L Tris–HCl, pH 7.5, and 1% Triton X-100). Extracts derived from supernatants were subjected to SDS–PAGE electrophoresis, and proteins were electrotransferred to nitrocellulose membranes. Immunodetection was performed using an ECL kit (Amersham) according to the manufacturer's instructions. Antibodies against 4-hydroxy-2-nonenal (4-HNE; Santa Cruz Biotechnology), Hsc70 (B-6; R&D Systems), Rad51, Brca2, Atm, Atr, Ku70, Ku80, and Msh2 (Cell Signaling Technology), and Angptl2 (3) were used.

Immunohistochemical staining

Skin tissues were fixed by perfusion with 4% paraformaldehyde in PBS (pH 7.4), washed in PBS for 15 minutes, dehydrated through a graded series of ethanols and xylene, and embedded in a single paraffin block. Sections (5 μm) were cut, air-dried, deparaffinized, and pretreated with 5 mmol/L periodic acid for 10 minutes at room temperature to inhibit endogenous peroxidase. Specimens were incubated for 1 hour with 50- to 100-fold diluted polyclonal antibody against Angptl2 (3) or Msh2 (Cell Signaling Technology), and then washed 3 times with PBS for 5 minutes. Sections were incubated with biotinylated anti-mouse IgG or anti-rabbit IgG (1:200 dilution; Vector Laboratories). Immunostaining was performed using the peroxidase-labeled avidin–biotin–complex method (1:100 dilution; DAKO). Sections were counterstained with hematoxylin.

DNA extraction and bisulfate modification

DNA was isolated from skin tissues using the SDS/proteinase K method. DNA concentration was determined spectrophotometrically at 260 nm. DNA bisulfite treatment was used to convert unmethylated CpG sites to UpG without modifying methylated sites, thus allowing them to be distinguished by restriction digestion using the Combined Bisulfite Restriction Analysis (COBRA) assay (17). Bisulfite treatment of genomic DNA was performed using the MethylEasy *Xceed* Rapid DNA Bisulphite Modification Kit (Human Genetic Signatures) according to the manufacturer's instructions. CpG-methylated NIH 3T3 mouse genomic DNA (New England Biolabs) served as a positive control and underwent bisulfite modification as described earlier. NIH 3T3 mouse genomic DNA (New England Biolabs) served as a negative control. The proportion of methylated versus unmethylated product (digested vs. undigested) was quantified by densitometry (23). Densitometric analysis was performed using Multi Gauge software (Fujifilm).

Published OnlineFirst November 20, 2013; DOI: 10.1158/1541-7786.MCR-13-0336

PCR and restriction digestion

Msh2 primers were specially designed for the COBRA assay as described previously (17). Sequences used were 5′-TGGCGGTGTAGTTTAAGGAGA-3′ (forward) and 5′-TCTTAAACACCTCGCGAACC-3′ (reverse), generating a 195-bp amplification product (17). PCR amplifications were performed using TaKaRa EpiTaq HS (for bisulfite-treated DNA; Takara Bio) according to the manufacturer's instructions. After amplification, PCR products were digested with *Mbo*I (Promega), which cuts DNA harboring a d (GATC) target site only if the site is retained after bisulfite-mediated deamination. Samples were separated on 2% agarose gels, which were then stained with ethidium bromide. The proportion of methylated versus unmethylated product (digested vs. undigested) was quantified by densitometry (17, 23) using MultiGauge version 3.1 software (Fuji Film).

Calculation of survival data

A Kaplan–Meier log-rank test was applied to analyze mouse survival data using JMP7 software (SAS Institute). A P value of less than 0.05 was considered significant.

Real-time quantitative RT-PCR

For mouse skin tissues, total RNA was isolated using the TRIzol reagent (Invitrogen). DNase-treated RNA was reverse transcribed with a PrimeScript RT reagent Kit (Takara Bio). PCR products were analyzed with a Thermal Cycler Dice Real Time system (Takara Bio), and relative transcript abundance was normalized to that of *18S* mRNA. PCR oligonucleotides were as follows: mouse *Msh2*: forward, 5′-GCCCAGGATGCCATTGTTAAAG-3′, reverse, 5′-AACGGGTGCTGCGTTTGAC-3′: mouse *18S*: forward, 5′-TTCTGGCCAACGGTCTAGACAAC-3′, reverse, 5′-CCAGTGGTCTTGGTGTGCTGA-3′: mouse *IL-1β*: forward, 5′-TCCAGGATGAGGACATGAGCAC-3′, reverse, 5′-GAACGTCACACACCAGCAGGTTA-3′: mouse *IL-6*: forward, 5′- CCACTTCACAAGTCGGAGGCTTA-3′, reverse, 5′- GCAAGTGCATCATCGTTGTTCATAC-3′. Results were analyzed using the two-tailed Student t-test with Excel software (Microsoft). A P value of less than 0.05 was considered significant.

Clinical characterization of patients

For ANGPTL2 and MSH2 immunostaining, we obtained normal abdominal skin tissues, as well as tissues derived by curative resection from patients with actinic keratosis and squamous cell carcinoma on the face (at Kumamoto University). Diagnostic evaluation of human samples was carried out by two independent dermatologists clinically and histologically. All studies were approved by the Ethics Committee of Kumamoto University. Written informed consent was obtained from each subject.

Results

Increased oxidative stress parallels Angptl2 expression in mouse skin tissues

Initially, we confirmed our previous findings regarding differences in susceptibility to chemically induced carcinogenesis among K14-*Angptl2* Tg, wild-type, and *Angptl2* KO mice by estimating the frequency and time course of SCC development in mice of all three genotypes. As we previously reported, increased Angptl2 expression in skin tissues accelerated carcinogenesis in the SCC model (Fig. 1A), whereas Angptl2 loss antagonized carcinogenesis (Fig. 1B). Seven weeks after initiation of chemical treatment, K14-*Angptl2* Tg, *Angptl2* KO, and respective wild-type mice showed little evidence of papillomas or SCC in chemically treated skin

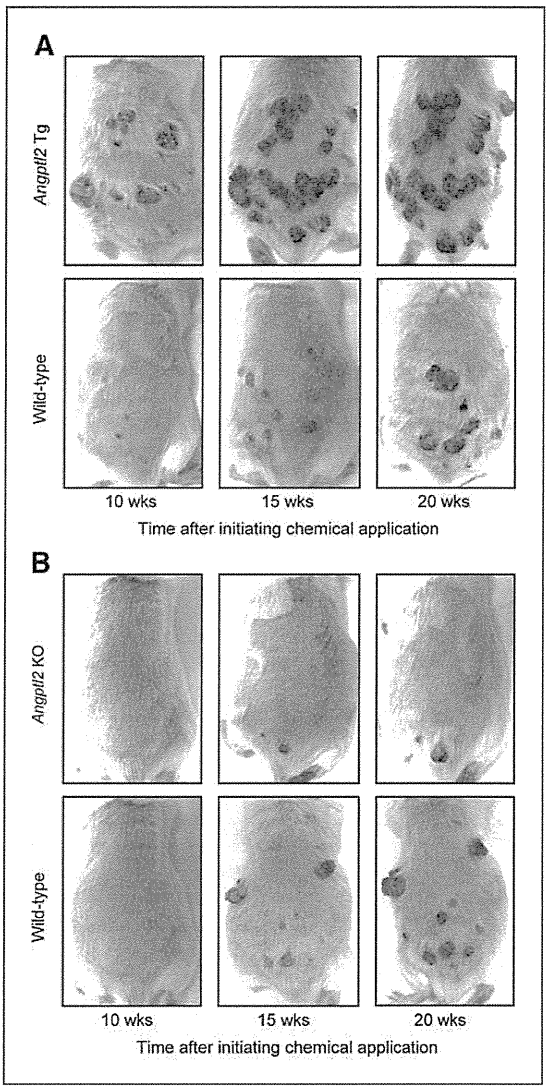

Figure 1. Chemical skin carcinogenesis is accelerated in skin tissues constitutively expressing Angptl2 and suppressed in *Angptl2*-deficient tissues. A and B, representative photographs showing the same mouse (in each row) throughout the time course of chemical skin carcinogenesis from both K14-*Angptl2* Tg and wild-type littermates (A) and *Angptl2* KO and wild-type littermates (B) at 10 (left), 15 (middle), and 20 (right) weeks after initiation of chemical application.